Proceedings of the International Conference Nanomaterials: Applications and Properties
Vol. **2** No 2, 02NNPA05(4pp) (2013)

Planar Superconducting Magnetic Flux Transformer with Micro- and Nanosized Branches

L.P. Ickitidze*, A.N. Mironyuk

National Research University «MIET», MIET, Zelenograd, 124498 Moscow, Russia

(Received 20 July 2013; published online 01 September 2013)

The object of the study is a superconducting film magnetic flux transformer comprising two square shaped loops with the tapering active strips and a magnetosensitive film element between them. It is shown that splitting of the active strips into parallel micro- and nanosized superconducting branches and slits increases the gain factor of the transformer, i. e., the concentration of an external magnetic field on the magnetosensitive element, by a factor of more than six.

Keywords: Magnetic flux transformer, Superconducting film, Factor of multiplication (concentration), Micro- and nanosized branches and slits, Magnetosensitive element, Giant magnetoresistance, Magnetic field sensor.

PACS numbers: 74.81.Fa, 74.50. + r, 74.25.Op, 74.72. – h, 85.75.Ss, 07.55.Ge, 85.25.Cp, 98.80.Bp

1. INTRODUCTION

Weak magnetic fields ($B \leq 10$ pT) are currently measured by different magnetometers [1-4]: SQUIDs (superconducting quantum interference devices), atomic, optical magnetometers, etc. The most sensitive of them are SQUIDs based on the effect of superconducting electrons tunneling through a weak link (Josephson junction or transition), but they do not measure the absolute value of a magnetic field and only detect changes in it. For SQUIDs, the magnetic field resolution δB, i.e., the minimum detectable magnetic field, is ~1 fT.

As the magnetosensitive element (MSE), any materials with sufficient nonlinearity of their magnetic characteristic can be used, for example, Hall sensors, materials and structures based on the effect of giant magnetoresistance (GMR), and granular or ceramic high-temperature superconducting (HTS) ma-terials. However, in order to improve the important parameters of a magnetic field sensor, in particular, to reduce δB, it is necessary to use concentrators of a measured (external) magnetic field that are called the magnetic flux transformers (MFTs). For this purpose, the property of superconductors to preserve the magnetic flux in a closed circuit without loss is often used.

The MFT elements based on HTS film materials are used in many magnetometers, where MSEs are SQUIDs [5], Hall sensors [6], sensors based on the GMR effect [7], sensors based on the magneto-resistive effect in ceramic HTS materials [8-10], etc.

As was shown in studies [11-13], the efficiency of the MFT can be increased by optimal fragmentation of its active strips into numerous parallel micro-, submicro-, and nanosized branches and slits. In this case, the MFT is separated from the MSE by an insulator film and concentrates an external magnetic field in the direction parallel to the substrate surface. In this work, we present the results of the calculations of the MFTs based on HTS film materials in a magnetic field sensor (MFS). Superconducting film loops serve as the MFT; as the MSE, different magnetoresistive elements can be used. The MFT and MSE lie in one plane and are separated from one another by gaps; a magnetic field to be measured is concentrated in the direction perpendicular to the substrate surface. We investigate the possibility of improving the important parameters of the MFT by local fragmentation of its active strips into numerous parallel superconducting branches and slits at a technological linewidth resolution of 100 ÷ 10000 nm.

2. MATERIALS AND METHODS

The object of the study is the factor F of the effective concentration of a magnetic field on the MSE for the case when the HTS-film-based MFT and the MSE lie in one plane and do not intersect. To increase F, the MFT active strips were split into several parallel branches in the areas adjacent with the MSE. The MFT was calculated with regard to the size effect when the current distribution in superconducting films significantly depends on their width. The following condition is satisfied for all superconducting films: the superconducting film width is much more than λ^2/h, where λ – the London penetration depth of the magnetic field, h – the superconducting film half-thickness.

The MFT comprises two active strips with the MSE symmetrically positioned between them (see Fig. 1a and Fig. 1b).

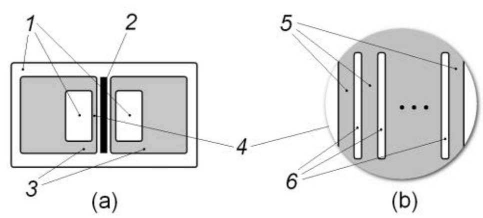

Fig. 1 – Layout of the MFT and MSE: (a) substrate – 1, MSE – 2, and superconducting MFT loops – 3; (b) MFT active strip consisting of numerous branches – 4 (enlarged). The shaded and unshaded areas show superconducting branches – 5, and slits – 6, respectively

*leo852@inbox.ru

The value of the factor F of the effective concentration of a magnetic field on the MSE is estimated as follows. In an external magnetic field B the magnetic flux shielded by the MFT loop 3 is calculated as: $\phi = A \cdot B$, where A – the MFT loop area. The screening current value I_S is calculated as: $I_S = \phi/(L+M)$, where L – the MFT loop inductance, M – the sum of the mutual inductances between the right and left loop, and also between the loops and MSE. It is known that the value of L is one (or more) order of magnitude larger than the total mutual inductance M.

The MFT active strip width w_s is one (or more) order of magnitude smaller than the width of the other MFT parts. This results in a substantial growth of the screening current density and thus the increase of the B concentration in the neighborhood of the MFT active strip and on MSE.

The MFT loop inductance is mainly determined by the inductance L of the MFT active strip. In the case when the latter is split into several branches, each with the inductance L_i $(i = 1,2,..., j$, where j, $n = j-1$ – the number of superconducting branches and slits in the MFT active strip, respectively). The fragmentation of the MFT active strip can increase L_j by no more than 15% which was not considered.

In an external magnetic field in the MFT active strip branches induced are the screening currents I_{Si} ($\sum_{i=1}^{j} I_{Si} = I_S$), flowing in the vicinity of MSE and influencing it by the magnetic field $B_{i\perp}$ in the point (x_0,y_0) inside MSE. The reference point (0,0) is located in the centre of the i-th branch upper surface. The value of $B_{i\perp}$ is calculated by formula:

$$B_{i\perp} = \frac{\mu_0 \cdot I_{Si}}{8\pi \cdot \lambda \cdot h} \cdot [\int_{-2h}^{0} \int_{-l}^{0} \frac{e^{-\frac{x+l}{\lambda}} \cdot (x_0 - x)}{(y_0 - y)^2 + (x_0 - x)^2} dxdy + \int_{-2h}^{0} \int_{0}^{+l} \frac{e^{-\frac{l-x}{\lambda}} \cdot (x_0 - x)}{(y_0 - y)^2 + (x_0 - x)^2} dxdy], \qquad (1)$$

where $l = w_{bi}/2$ and h are the i-th branch half-width and half-thickness, respectively, $\mu_0 = 4\pi \cdot 10^{-7}$ H/m – the magnetic constant, $I_{Si}/4\lambda h \le J_c$, J_c – the critical current density for the film of MFT. In all cases it is supposed that the length of the branches significantly exceeds w_{bi} and the technological linewidth resolution w_a. In the calculations considered were: $B_\perp(j) = 2\sum_{i=1}^{j} B_{i\perp}$, where $B_{i\perp}$ was calculated by formula (1); $<B_\perp(j)>$ – the value of $B_\perp(j)$ averaged along the MSE width w_0; the rectangular quadrature method was used for numerical integration.

The relative gain factor F, which is calculated with no regard to the change in the resulting inductance of branches, is calculated as:

$$F = \frac{<B_\perp(j)>}{<B_\perp(j=1)>}, \qquad (2)$$

where $<B_\perp(j=1)>$ – the magnetic field averaged along the MSE width w_0 for the case of j=1 (i.e., the unsplit MFT active strip).

In all the calculations with the use of formulas (1)-(2), it was assumed that slit width w_p coincides with technological linewidth resolution w_a. Width w_s of the MFT active strip and widths w_{bi} of its branches were assumed to be multiple of w_a. For the specified values of w_a, we determined the optimal splitting of the MFT active strip into branches for attaining the maximum value of F ($F_{\max}$).

3. DISCUSSION OF RESULTS

The calculations were made for the two variants: the active MFT strip widths are w_s=30 μm, w_0=10 μm (variant 1) and w_s = 3 μm, w_0 = 1 μm (variant 2). The value of λ varies between 50 and 250 nm in 50 nm increments, and the table data are given for 50 and 250 nm.

Variant 1. Table 1 gives the values of $F_{\max}$ for the optimal splitting of the MFT active strip into branches at $w_p = w_a$ = 1, 2, 5, and 10 μm. Slits (w_p) and branches (w_{bi}) start alternating from the gap between the MFT and the MSE. The slit widths are given with bold italics and the superconducting branch widths – with the regular type.

In the calculations, the following values were used: J_c = 10^{10} A/m^2, h = 10 nm, w_s = 30 μm, w_0 = 10 μm, and width of the gap between the MFT and MSE w_g = 1 μm.

As the value of w_p is decreased, the number of branches and slits corresponding to the optimal splitting grows and the maximum values of the MFT gain factor increases.

Table 1 – Parameters of the MFT with the optimal splitting of its active strip into superconducting branches and slits (variant 1)

λ, nm	$w_p = w_a$, μm	Optimal splitting w_{bi}, μm	$F_{\max}$
50	1	1-***1***-1-***1***-1-***1***-1-***1***-1-***1***- -1-***1***-1-***1***-1-***1***-1-***1***-12	6.48
	2	2-***2***-2-***2***-2-***2***-2-***2***-14	3.44
	5	5-***5***-20	1.62
	10	10-***10***-10	1.40
250	1	1-***1***-1-***1***-1-***1***-1-***1***-1-***1***- -1-***1***--2-***1***-2-***1***-2-***1***-9	5.97
	2	2-***2***-2-***2***-2-***2***-2-***2***-14	3.52
	5	5-***5***-20	1.66
	10	10-***10***-10	1.42

It can be seen that the efficiency of the concentration of a magnetic field on the MSE grows with the number of branches in the MFT active strip: at λ = 50 nm for 2 branches, the concentration grew by 40% relative to the unsplit MFT strip and for 10 branches – by 54%. It should be noted that the optimal splitting can be with different branch widths; at a large number of branches, their widths will strongly differ; e.g., at λ = 50 nm and w_p = 1 μm, the first branch width is w_{b1} = 1 μm and the tenth branch width is w_{b10} = 12 μm. It is important that at the optimal splitting the branch width can grow or remain invariable but cannot decrease with increasing distance from the MSE.

The results presented here were computed by enumerating possible variants of the splitting of the MFT active strip into branches (in particular, ≈$8\cdot10^5$ variants for w_p = w_a = 1 μm), which required substantial computational burden. Further decrease in w_p at a fixed value of the MFT active strip width w_s will undoubtedly lead to even larger computer resource consumption.

According to the calculation procedure, in order to optimize the computation time – first, averaged concentrations of a magnetic field on the MSE were calculated by formula (1) for all possible locations and widths of branches at specified technological parameters (λ, w_s, w_0, w_a, etc.). Then, the variants of the splitting of the MFT active strip were enumerated to choose the optimal variant corresponding to the maximum concentration of a magnetic field on the MSE with regard to the change in the resulting inductance of branches. The combinatorial growth of the number of splitting variants does not allow us to consider this algorithm to be universal. To optimize the computational algorithm, further investigations are needed.

Variant 2. In the second variant of the calculations, in order to improve the important parameters of the sensor (in particular, to reduce δB), we studied the possibility of the transition to the nanosized technological linewidth resolution. In the calculations, we used the following values: J_c = 10^{10} A/m^2, h = 10 nm, w_p = w_a = 100, 200, 500, and 1000 nm. In contrast to variant 1, the following widths differ: w_s = 3 μm, w_0 = 1 μm, and w_g = 100 nm. Table 2 gives the values of $F_{\max}$ for the optimal splitting of the MFT active strip into branches at w_p = 100, 200, 500, and 1000 nm. The slit widths (nm) are given with bold italics and the superconducting branch widths – with the regular type. As before, with decreasing w_p the number of branches and slits corresponding to the optimal splitting grows and the maximum values of the resulting MFT gain factor increases.

Table 2 – Parameters of the MFT with the optimal splitting of its active strip into superconducting branches and slits (variant 2)

λ, nm	$w_p = w_a$, nm	Optimal splitting w_{bi}, nm	$F_{\max}$
50	100	100-***100***-200-***100***-200--***100***-200-***100***-200-***100***--200-***100***-300-***100***-300--***100***-500	4.83
	200	200-***200***-200-***200***-200--***200***-400-***200***-1200	3.31
	500	500-***500***-2000	1.7
	1000	1000-***1000***-1000	1.44
250	100	300-***100***-300-***100***-300--***100***-300-***100***-400-***100***--400-***100***-400	2.51
	200	400-***200***-600-***200***-600--***200***-800	2.09
	500	500-***500***-2000	1.47
	1000	1000-***1000***-1000	1.43

It can be seen that the efficiency of the concentration of a magnetic field on the MSE grows with the number of branches in the MFT active strip: at λ = 50 nm for 2 branches, $F_{\max}$ grew by 44% relative to the case of the unsplit MFT strip and at 9 branches – by 383%.

The comparison of $F_{\max}$ values for the two variants (see Table 1 and Table 2) shows that they have the same order of magnitude and are not significantly different. This implies that if we miniaturize the geometric dimensions of MFS by a scale factor of 10 (variant 1: w_s = 30 μm, w_0 = 10 μm, w_g = 1 μm; variant 2: w_s = 3 μm, w_0 = 1 μm, w_g = 100 nm), it does not have a substantial effect on the value of $F_{\max}$.

Fig. 2 shows the layout of the MFT branches and MSE strip for 9 branches in the relative scale according to their optimal sizes and location calculated at the following parameters: λ = 50 nm, J_c = 10^{10} A/m^2, h = 10 nm, w_s = 3 μm, w_0 = 1 μm, w_g = 100 nm, and w_p = w_a = 100 nm.

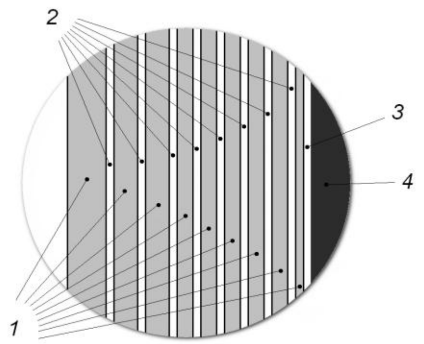

Fig. 2 – Optimal splitting of the MFT active strip at the initial parameters (variant 2, λ = 50 nm, J_c = 10^{10} A/m^2): (1) – MFT active strip branches, (2) – slits, (3) – gap between MFT and MSE, (4) MSE – strip. (The numerical width values for the depicted optimal splitting are given in Table 2, row 1)

The results obtained can be used for estimating possible enhancement of the efficiency of the weak magnetic field sensor considered in [7], in which a material with the GMR effect was used as the MSE and an HTS Y-Ba-Cu-O film was used as the MFT. In this sensor, the active MFT strip width is 1 μm and, according to the data given in Table 2 (case λ = 250 nm, $w_p = w_a = 100$ nm), at the optimal splitting of its MFT active strip the gain factor of the sensor will grow by more than 100%. One may expect that the magnetic field resolution δB will correspondingly decrease and the dynamic range of the MFS will broaden.

4. CONCLUSIONS

The analysis of the obtained results shows that fragmentation of the MFT active strips into nanosized superconducting branches and slits (the slit width lies within ~100 – 10000 nm) makes it possible to increase the MFT gain factor and, correspondingly, the concentration of an external magnetic field on the MSE, by a factor of more than 6 in the case of a wide (~10 μm) MSE and by more than 4 in the case of a narrow (~1 μm) one.

The value of $F_{\max}$ can be further increased by decreasing the gap between the MFT active strips and the MSE or by using the materials with high J_c and low λ, e.g., niobium films as the MFT. Indeed, in niobium heteroepitaxial layers (NHEL) on sapphire substrates (highly textured, nearly single-crystal) at the temperature $T \sim 4K$ the values $J_c \sim 10^7$ A/cm^2 and λ ~ 50 nm are attained [13, 14]. The choice of the NHEL as the MFT will apparently lead to the growth of $F_{\max}$ by more than an order of magnitude relative to the considered here HTS materials with the values $J_c \sim 10^6$ A/cm^2 and λ ~ 200-250 nm. The niobium films have already demonstrated their higher efficiency (higher values of F) as compared to the films in the Y-123 system when used as a material for the MFT with continuous active strips [7]. Certainly, the growth of F and $F_{\max}$ will ensure the reduction of the magnetic field resolution of the MFS (~1/F) [11-12] for detecting weaker magnetic fields.

The structure of MFS considered in this work is planar: the MFT and MSE lie in one plane and do not intersect. Consequently, such a single-layer film sensor of weak magnetic fields is much easier to fabricate as compared to the multilayer structures often used in SQUIDs.

At present, there are no high-temperature superconductors that would allow connecting their ends so that the closed ring had no superconductivity (magnetic flux) loss and could serve as the MFT element. We believe that the magnetic flux transformer based on superconductivity films with the nanostructured active strips will facilitate solving the above-mentioned problem [15].

ACKNOWLEDGEMENT

This study was partially supported by the Ministry of Education of the Russian Federation (state contract № 14.513.12.002 from 28.02.2013, agreement 14.B37.21.0567) and by the Foundation for Promotion of Small Enterprises in Science and Technology (contract 10678p/19537).

The authors thank Professor S.V. Selishchev for the support of this study.

REFERENCES

1. D. Robbes, *Sensor. Actuat. A-Phys.* **129**, 86 (2006).
2. I.K. Kominis, T.W. Kornack, J.C. Allred, and M.V. Romalis, *Nature* **422**, 596 (2003).
3. T.H. Sander, J. Preusser, R. Mhaskar, J. Kitching, L. Trahms, S. Knappe, *Biomed. Opt. Express* **3** No5, 981 (2012).
4. J. Deak, A.H. Miklich, J. Slonczewski, R.H. Koch, *Appl. Phys. Lett.* **69** No8, 1157 (1996).
5. J.M. Jaycox, M.B. Ketchen, *IEEE Trans. Magn.* **MAG-17**, 400 (1981).
6. S. Linzen, F. Schmidt, F. Schmidl, *Physica C* **372-376**, 146 (2002).
7. M. Pannetier, C. Fermon, G. Le Goff, *Science* **304 (5677)**, 1648 (2004).
8. L.P. Ichkitidze, *Patent RU* 2289870.
9. L.P. Ichkitidze, *Physica C* **435**, 140 (2006).
10. L.P. Ichkitidze, *Physica C* **460-462**, 781 (2007).
11. L.P. Ichkitidze, A.N. Mironyuk, *Physica C* **472**, 57 (2012).
12. L.P. Ichkitidze, A.N. Mironyuk, *J. Phys. Conf. Ser.* **400(2)**, 022032 (2012).
13. L.P. Ichkitidze, V.I. Skobelkin, R.A. Bablidze, and V.P. Kuznetsov, *Fizika Nizkih Temperatur (USSR)* **12(5)**, 474 (1986).
14. L.P. Ichkitidze, V.I. Skobelkin, R.A. Bablidze, *Fizika Tverdogo Tela (USSR)* **27(10)**, 474 (1986).
15. N.V. Porohov, E.E. Levin, M.L. Chuharkin, *J. Commun. Technol. El.* **57(10)**, 1128 (2012).